A Low Complexity Multiuser Interference Compensation Scheme for OFDMA Uplink

Yang Zhang, Jiandong Li, Lihua Pang, and Qin Liu
State Key Laboratory of Integrated Service Networks, Xidian University, Xi'an 710071, China
E-mail: yangzhang1984@gmail.com

***Abstract*—This paper investigates the multiuser interference mitigation for the uplink of an orthogonal frequency division multiple access system in a doubly selective fading channel. The proposed algorithm squeezes the interference of subcarrier k into $2\tau+1$ neighboring subcarriers by preprocessing the received signal and yields a banded structure interference matrix. Specifically, the value of τ mainly depends on the carrier frequency offsets and determines the squeezing depth which in turn influences the receiver implementation complexity. Simulation results show that the bit error rate performance of our proposed algorithm approaches the existing full length minimum mean square error equalizer with a significant reduction on complexity.**

I. INTRODUCTION

ORTHOGONAL frequency division multiple access (OFDMA) features its intrinsic flexibility in resource allocation and multiuser diversity exploitation. One major disadvantage is its sensitivity to frequency asynchronism. A misadjusted oscillator or the presence of Doppler will induce carrier frequency offsets (CFOs) and destroy the orthogonality among subcarriers, leading to intercarrier interference (ICI). In OFDMA systems, the ICI induced by other users is generally referred to as multiple user interference (MUI). Mitigating ICI in an OFDMA uplink is challenging since it cannot be accomplished by merely compensating the CFO for each user.

In early works, the main concern is on the frequency synchronization recovery [1], where users' CFOs are estimated at the receiver and sent back to transmitter via a downlink control channel for carrier frequency adjustment. To mitigate the ICI caused by the residual CFO, a user detection scheme is usually employed to improve system performance without feedback delay and extra overhead. The single user detector analyzed in [2] is the earliest detection scheme used in OFDMA systems. The main disadvantage is its high computational complexity due to the use of multiple fast Fourier transform (FFT) modules. To tackle with the complexity, the authors in [3] designed a variant detector in which circular convolution is employed to suppress ICI after FFT. Since both these schemes simply perform CFO compensation for each user without any concern given for MUI removal, the performance is limited by an irreducible error floor. In [4]-[6], successive interference suppression, parallel interference suppression and minimum mean square error (MMSE) schemes have been exploited for OFDMA systems. MMSE equalization requires $O(N^3)$ computations [7], where N is the total number of orthogonal subcarriers. In [8] the interference generated by subcarrier k is localized to its $k\pm\tau$ neighboring subcarriers and the interference on the remaining subcarriers is neglected. The complexity of the algorithm is $O(N(\tau^2+1))$, here the value of τ increases with the deterioration of CFOs. Taking advantage of an interleaved OFDMA structure, [9] partitions the whole system into several smaller subsystems, after which the MMSE technique is applied to the subsystems. This method requires low complexity and gives reliable performance. However, it is only applicable to an ideal interleaved structure. More recent study [10] has proposed a low complexity zero-forcing (ZF) compensation scheme which employs Newton's method with FFTs to solve matrix inversion iteratively. The complexity of this algorithm is reduced from $O(N^3)$ to $O(2N\log_2 N)$.

However, a common assumption in these studies is that multipath fading channels are invariant within each OFDMA block. In the latest IEEE 802.16e standard, it is necessary for OFDMA to support mobile communications at speeds of up to 120 km/h. Different from static channels, ICI mitigation in time and frequency selective fading channels involves equalization because ICI is partially caused by channel variations. In [11], the effect of Doppler spread on ICI in the OFDMA uplink has been analyzed. However, mitigation of the ICI induced by channel variations has not been explicitly addressed. Until recently, Hou [12] investigated the ICI suppression for the uplink of OFDMA systems in doubly selective fading channels, but unfortunately, the proposed detection schemes still entail prohibitively high complexity.

We study the low complexity ICI suppression technique for the OFDMA uplink in time and frequency selective fading channels. Based on the signal model formulated, instead of ignoring some interference terms as in [8], we squeeze them into only $2\tau+1$ interference terms (a limited span). To do this, the received samples are circularly convolved with coefficients of the preprocessing filter designed to maximize the signal to interference plus noise ratio (SINR). Squeezing the interference of subcarrier k into $2\tau+1$ samples also compresses the contribution of the transmitted symbol at subcarrier k into $2\tau+1$ received samples. Consequently, only $2\tau+1$ received samples are used to estimate the transmitted symbol at subcarrier k using the MMSE equalizer of the same length.

II. SIGNAL MODEL

Consider the uplink of an OFDMA system with U users simultaneously communicating with the base station (BS) through independent time and frequency selective fading channels. At the transmitter of user u, information symbols are grouped and padded with zeros to form a block $[X_u(0), X_u(1), \cdots, X_u(N-1)]$, which is then fed into an inverse FFT (IFFT) modulator. In the resulting OFDMA block, information symbols are located on the associated subcarriers,

This work is supported by the National Basic Research Program of China (2009CB320404), the National Nature Science Foundation of China (60902033, 60972047), the 111 Project (B08038) and the Program for Changjiang Scholars and Innovative Research Team in University (IRT0852).

978-1-4673-0990-5/12/$31.00 ©2012 IEEE

while zero symbols are placed on the subcarriers employed by other users. A cyclic prefix (CP) is appended at the beginning of each OFDMA block to form a guard interval. Hence, the signal transmitted from user u is given by

$$x_u(n) = \frac{1}{\sqrt{N}} \sum_{k=0}^{N-1} X_u(k) \mathrm{e}^{j2\pi nk/N} \qquad -N_g \le n \le N-1 \tag{1}$$

where N_g is the length of CP. The channel model is a wide sense stationary uncorrelated scattering time varying multipath fading channel with a delay spread L. The signal received from user u can be mathematically described as

$$\begin{aligned} r_u(n) &= \sum_{l=0}^{L-1} h_u(n,l) x_u(n-l) + z(n) \\ &= \frac{1}{\sqrt{N}} \sum_{k=0}^{N-1} X_u(k) \overline{H}_u(n,k) \mathrm{e}^{j2\pi nk/N} + z(n) \end{aligned} \tag{2}$$

where $h_u(n,l)$ stands for the channel impulse response (CIR) of path l at time n, and $\overline{H}_u(n,k) = \sum_{l=0}^{L-1} h_u(n,l) e^{-j2\pi lk/N}$ is the frequency response of subcarrier k at time n. $z(n)$ is a complex white noise with variance σ_z^2. At the receiver, due to clock and local oscillator misalignment between the BS receiver and the transmitter, a time offset and a CFO are induced into the baseband signal. Therefore, (2) can be reformulated as

$$r_u(n) = \frac{1}{\sqrt{N}} \sum_{k=0}^{N-1} X_u(k) \overline{H}_u(n,k) \mathrm{e}^{j2\pi (n-n_u)(k+\varepsilon_u)/N} + z(n) \tag{3}$$

where n_u and ε_u are the time offset and CFO normalized with respect to the sampling period and the subcarrier spacing, respectively. In the ensuing discussions, we will use ε_u only for the CFO caused by a misadjusted local oscillator, noting that the CFO incurred by channel variations, as will be shown later, has been included in the channel modeling. In practice, a coarse time and frequency synchronization would have been accomplished before the commencement of data transmission. As a result, the time and frequency offset considered here are their residual values and usually appear as a fraction of the sampling period and the subcarrier spacing. Since the fractional time offset only arouses a linear phase shift across the channel frequency responses and can be compensated for in equalization, synchronization for such a time offset is not needed [12]. By combining the fractional time offset into the channel frequency response, the baseband signal given by (3) can be rewritten as

$$r_u(n) = \frac{1}{\sqrt{N}} \sum_{k=0}^{N-1} X_u(k) H_u(n,k) \mathrm{e}^{j2\pi n(k+\varepsilon_u)/N} + z(n) \tag{4}$$

where $H_u(n,k) = \overline{H}_u(n,k) e^{-j2\pi n_u(k+\varepsilon_u)/N}$. From (4), the multiuser signal received from all the users is given by

$$r(n) = \sum_{u=1}^{U} e^{j2\pi n\varepsilon_u/N} \sum_{k=0}^{N-1} \frac{\mathrm{e}^{j2\pi nk/N}}{\sqrt{N}} X_u(k) H_u(n,k) + z(n) \tag{5}$$

Consequently, each received OFDMA block can be expressed in a more compact matrix form as

$$\boldsymbol{r} = \sum_{u=1}^{U} \boldsymbol{D}_u \boldsymbol{H}_u \boldsymbol{M}_u \boldsymbol{X} + \boldsymbol{z} \tag{6}$$

where $\boldsymbol{D}_u = diag(1, e^{j2\pi\varepsilon_u/N}, \cdots, e^{j2\pi(N-1)\varepsilon_u/N})$, $\boldsymbol{H}_u$ is given by (7) shown at the top of the next page, $\boldsymbol{M}_u$ is described by

$$[\boldsymbol{M}_u]_{i,j} = \begin{cases} 1, & i = j \quad and \quad X_u(i) \ne 0 \\ 0, & otherwise \end{cases} \tag{8}$$

and $\boldsymbol{X} = [X(0), X(1), \cdots, X(N-1)]^T$ contains information symbols on all the subcarriers. These symbols may belong to different users, depending on the specific carrier assignment scheme (CAS) employed by the OFDMA uplink. The vector $\boldsymbol{z}$ in (6) represents background noise. When the channel is static or quasi-static, the signal model given by (6) will degenerate to become

$$\boldsymbol{r} = \left(\sum_{u=1}^{U} \boldsymbol{D}_u \boldsymbol{F} \boldsymbol{M}_u \right) \boldsymbol{H} \boldsymbol{X} + \boldsymbol{z} \tag{9}$$

where $\boldsymbol{H} = diag(H(0), H(1), \cdots, H(N-1))$ denotes the channel frequency response matrix in which $H(k)$ is associated with the designated user that occupies subcarrier k and $[\boldsymbol{F}]_{i,j} = 1/\sqrt{N}\, e^{j2\pi ij/N}$ represents the element of the unitary IFFT matrix, respectively. By comparing (6) and (9), we find that unlike the situation in static and quasi-static channels, ICI mitigation in a time selective scenario involves channel equalization. Finally, applying the FFT on (6) the frequency domain received multiuser signal vector can be written as

$$\boldsymbol{R} = \sum_{u=1}^{U} \boldsymbol{F}^H \boldsymbol{D}_u \boldsymbol{H}_u \boldsymbol{M}_u \boldsymbol{X} + \boldsymbol{F}^H \boldsymbol{z} = \sum_{u=1}^{U} \boldsymbol{A}_u \boldsymbol{M}_u \boldsymbol{X} + \boldsymbol{Z} \tag{10}$$

where $[\boldsymbol{A}_u]_{i,j} = 1/N \sum_{n=0}^{N-1} H_u(n,j) e^{j2\pi n(\varepsilon_u + j - i)/N}$ and the off-diagonal elements of $\boldsymbol{A}_u$ can be regarded as ICI terms. Again, we will investigate two special cases: if the CIR remains constant within each OFDMA block, the presence of CFO caused by local oscillator misalignment renders the ICI matrix $\boldsymbol{I}_u = \boldsymbol{F}^H \boldsymbol{D}_u \boldsymbol{F}$ defined in (9) a symmetric structure with entity

$$[\boldsymbol{I}_u]_{i,j} = \frac{1}{N} \frac{1 - e^{j2\pi(j-i+\varepsilon_u)}}{1 - e^{j2\pi(j-i+\varepsilon_u)/N}}, 0 \le i, j \le N-1 \tag{11}$$

Furthermore, if $\varepsilon_u = 0$ then there is no ICI and $\boldsymbol{I}_u$ degenerates into an identity matrix [13]. The proposed algorithm can be used for any CAS, but in this work only interleaved CAS is considered for easy understanding. Therefore, the received signal using interleaved CAS can be written as

$$\boldsymbol{R} = \boldsymbol{A}\boldsymbol{S} + \boldsymbol{Z} \tag{12}$$

where $\boldsymbol{A}$ and $\boldsymbol{S}$ are defined in (13) and (14) respectively, while $a_{i,j}^u = [\boldsymbol{A}_u]_{i,j}$. Fig. 1 shows the amplitudes of the ICI terms produced by subcarrier 0 on nearby subcarriers with respect to different mobile scenarios. The simulation parameters are depicted in Section IV. It is observed that the faster the user moves, the more ICI power will be incurred. Due to the periodical property of FFT, the interference imposed on the first and last portions of subcarriers, which are neighboring to subcarrier 0, is significant.

III. Interference Mitigation

The ICI suppression can be either linear or nonlinear. Specifically, we will focus on the MMSE technique which

$$\boldsymbol{H}_u = \frac{1}{\sqrt{N}} \begin{bmatrix} H_u(0,0) & H_u(0,1) & \cdots & H_u(0,N-1) \\ H_u(1,0) & H_u(1,1)e^{j2\pi/N} & \cdots & H_u(1,N-1)e^{j2\pi(N-1)/N} \\ \vdots & \vdots & \ddots & \vdots \\ H_u(N-1,0) & H_u(N-1,1)e^{j2\pi(N-1)/N} & \cdots & H_u(N-1,N-1)e^{j2\pi(N-1)^2/N} \end{bmatrix} \tag{7}$$

$$\boldsymbol{A} = \begin{bmatrix} a_{0,0}^1 & \cdots & a_{0,U-1}^U & a_{0,U}^1 & \cdots & a_{0,N-1}^U \\ a_{1,0}^1 & \cdots & a_{1,U-1}^U & a_{1,U}^1 & \cdots & a_{1,N-1}^U \\ \vdots & \cdots & \vdots & \vdots & \cdots & \vdots \\ a_{N-1,0}^1 & \cdots & a_{N-1,U-1}^U & a_{N-1,U}^1 & \cdots & a_{N-1,N-1}^U \end{bmatrix} \tag{13}$$

$$\boldsymbol{S} = [X_1(0), \cdots, X_U(U-1), X_1(U), \cdots, X_U(N-1)]^T \tag{14}$$

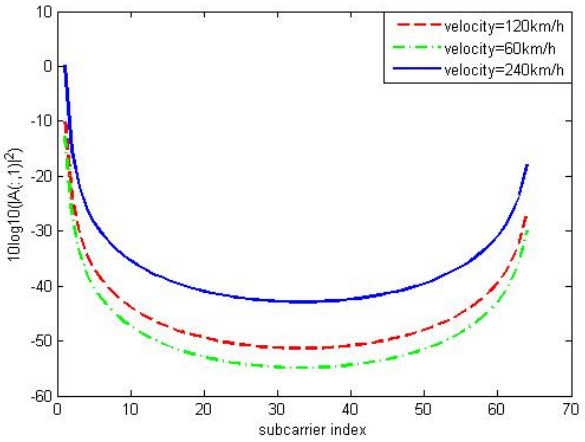

Fig. 1. The power of interference on the nearby subcarriers in the first column of the matrix $\boldsymbol{A}$ with respect to different mobile scenarios.

attempts to remove both interference and noise and therefore avoids severe noise enhancement. The MMSE equalizer is derived as follows, assuming $\mathrm{E}(\boldsymbol{S}) = \mathrm{E}(\boldsymbol{Z}) = \boldsymbol{0}$, $\mathrm{E}(\boldsymbol{S}\boldsymbol{S}^H) = \sigma_s^2 \boldsymbol{I}$, $\mathrm{E}(\boldsymbol{S}\boldsymbol{Z}^H) = \boldsymbol{0}$ with σ_s^2 being the power allocated on each subcarrier,

$$\hat{\boldsymbol{S}} = \boldsymbol{A}^H \left(\frac{\sigma_z^2}{\sigma_s^2}\boldsymbol{I} + \boldsymbol{A}\boldsymbol{A}^H\right)^{-1} \boldsymbol{R} \tag{15}$$

With identical time invariant channels as well as perfect oscillator synchronizations of all involved users, $\boldsymbol{A}$ is diagonal, and (15) can be implemented in $O(N)$ computations. While in our scenario, (15) requires $O(N^3)$ operations to invert a matrix, thus restricting its use to small N OFDMA systems. In order to decrease the equalizer complexity, we preprocess the frequency domain received signal samples to squeeze the ICI response of $\boldsymbol{A}$ into the $2\tau+1$ central diagonals, a $\tau \times \tau$ lower triangular matrix in the bottom left corner, and a $\tau \times \tau$ upper triangular matrix in the top right corner as illustrated by the shaded regions in [14-Fig. 4]. The parameter $\tau \in \{0,1,\cdots,N/2-1\}$ controls the target ICI response depth: larger τ corresponds to a longer ICI span and thus, increased estimation complexity.

We leverage the receiver's FFT operation to achieve ICI shortening via fast convolution. Therefore, the received ICI squeezed signal can be written as

$$C(\boldsymbol{\beta})\boldsymbol{R} = C(\boldsymbol{\beta})\boldsymbol{A}\boldsymbol{S} + C(\boldsymbol{\beta})\boldsymbol{Z} \tag{16}$$

where $C(\boldsymbol{\beta})$ denotes the circulant convolution matrix generated by the frequency domain filter coefficient vector $\boldsymbol{\beta}$. We expect that $C(\boldsymbol{\beta})\boldsymbol{A}$ has banded structure. In order to determine the value of $\boldsymbol{\beta}$, the matrix $C(\boldsymbol{\beta})\boldsymbol{A}$ is partitioned into the squeezed signal and interference parts as

$$C(\boldsymbol{\beta})\boldsymbol{A} = M_S(C(\boldsymbol{\beta})\boldsymbol{A}) + M_{ICI}(C(\boldsymbol{\beta})\boldsymbol{A}) \tag{17}$$

where M_S is the masking operator that selects the squeezed signal part and M_{ICI} chooses the ICI part. Therefore, using (17), (16) can be expressed as

$$C(\boldsymbol{\beta})\boldsymbol{R} = \underbrace{M_S(C(\boldsymbol{\beta})\boldsymbol{A})\boldsymbol{S}}_{signal} + \underbrace{M_{ICI}(C(\boldsymbol{\beta})\boldsymbol{A})\boldsymbol{S} + C(\boldsymbol{\beta})\boldsymbol{Z}}_{\text{int}\,erference+noise} \tag{18}$$

We anticipate that the value of $\boldsymbol{\beta}$ should maximize the energy of the signal part and minimize the energy of the ICI plus noise part. The total energy of the ICI squeezed received signal part ε_{total}, employing FFT property $\boldsymbol{F}C(\boldsymbol{\beta})\boldsymbol{F}^H = diag(\sqrt{N}\boldsymbol{F}\boldsymbol{\beta})$ and assuming $\boldsymbol{b} = \sqrt{N}\boldsymbol{F}\boldsymbol{\beta}$, is calculated as

$$\varepsilon_{total} = \left\|C(\boldsymbol{\beta})\boldsymbol{R}\right\|_F^2 = \boldsymbol{b}^H diag(\boldsymbol{F}(\sigma_s^2 \boldsymbol{A}\boldsymbol{A}^H + \sigma_z^2 \boldsymbol{I})\boldsymbol{F}^H)\boldsymbol{b} \tag{19}$$

Due to the adoption of the interleaved CAS, we define (20) and (21) shown at the top of the next page. The energy of the squeezed signal part ε_s can be evaluated as

$$\varepsilon_s = \frac{\sigma_s^2 \left\|M_S \boldsymbol{F}^H diag(\boldsymbol{b})\boldsymbol{E}\right\|_F^2}{N^2} = \frac{\sigma_s^2 \left\|M_S \boldsymbol{P}\right\|_F^2}{N^2} \tag{22}$$

By rearranging the elements of matrix $\boldsymbol{P}$ into a new matrix $\boldsymbol{G}$ such that $[\boldsymbol{G}]_{(i-j)_N,j} = [\boldsymbol{P}]_{i,j}$, where $(n)_N$ denotes n modulo N, i.e., $(n)_N$ is the remainder from dividing n by N, the diagonals can be converted into rows. Specifically, the main diagonal of $\boldsymbol{P}$ appears on the first row of $\boldsymbol{G}$, the first sub-diagonal on the second row, the first super-diagonal on the last row, and so on. With this substitution ε_s can be described as

$$\varepsilon_s = \frac{\sigma_s^2 \left\|\boldsymbol{\Delta}\boldsymbol{G}\right\|_F^2}{N^2} \tag{23}$$

where $\boldsymbol{\Delta} = \begin{bmatrix} \boldsymbol{I}_{\tau+1} & \boldsymbol{0} & \cdots & \boldsymbol{0} \\ \boldsymbol{0} & \boldsymbol{0} & \ddots & \vdots \\ \vdots & \ddots & \ddots & \boldsymbol{0} \\ \boldsymbol{0} & \cdots & \boldsymbol{0} & \boldsymbol{I}_\tau \end{bmatrix}$ and $\boldsymbol{G}$ are defined in (24). The squared absolute value of the l th element of $\boldsymbol{g}_k(\varepsilon_u)$ can be

$$\boldsymbol{E}=\left[\boldsymbol{e}_0(\varepsilon_1)\ \ \cdots\ \ \boldsymbol{e}_{U-1}(\varepsilon_U)\ \ \boldsymbol{e}_U(\varepsilon_1)\ \ \cdots\ \ \boldsymbol{e}_{N-1}(\varepsilon_U)\right]$$

$$\boldsymbol{e}_k(\varepsilon_u)=[H_u(0,k),H_u(1,k)e^{j2\pi(\varepsilon_u+k)/N},\cdots,H_u(N-1,k)e^{j2\pi(\varepsilon_u+k)(N-1)/N}]^T \tag{20}$$

$$\boldsymbol{P}=\left[\boldsymbol{p}_0(\varepsilon_1)\ \ \cdots\ \ \boldsymbol{p}_{U-1}(\varepsilon_U)\ \ \boldsymbol{p}_U(\varepsilon_1)\ \ \cdots\ \ \boldsymbol{p}_{N-1}(\varepsilon_U)\right]$$

$$\boldsymbol{p}_k(\varepsilon_u)=[\sum_{n=0}^{N-1}b_nH_u(n,k)e^{j2\pi(\varepsilon_u+k)n/N},\sum_{n=0}^{N-1}b_nH_u(n,k)e^{j2\pi(\varepsilon_u+k-1)n/N},\cdots,\sum_{n=0}^{N-1}b_nH_u(n,k)e^{j2\pi(\varepsilon_u+k-N+1)n/N}]^T \tag{21}$$

$$\boldsymbol{G}=\left[\boldsymbol{g}_0(\varepsilon_1)\ \ \cdots\ \ \boldsymbol{g}_{U-1}(\varepsilon_U)\ \ \boldsymbol{g}_U(\varepsilon_1)\ \ \cdots\ \ \boldsymbol{g}_{N-1}(\varepsilon_U)\right]$$

$$\boldsymbol{g}_k(\varepsilon_u)=[\sum_{n=0}^{N-1}b_nH_u(n,k)e^{j2\pi\varepsilon_un/N},\sum_{n=0}^{N-1}b_nH_u(n,k)e^{j2\pi(\varepsilon_u-1)n/N},\cdots,\sum_{n=0}^{N-1}b_nH_u(n,k)e^{j2\pi(\varepsilon_u-N+1)n/N}]^T \tag{24}$$

derived as

$$\left|\sum_{n=0}^{N-1}b_nH_u(n,k)e^{j2\pi(\varepsilon_u-l)n/N}\right|^2=\boldsymbol{b}^H\boldsymbol{J}_u^H\boldsymbol{D}_u^H\boldsymbol{e}^H(l)\boldsymbol{e}(l)\boldsymbol{D}_u\boldsymbol{J}_u\boldsymbol{b} \tag{25}$$

where $\boldsymbol{e}(l)=[1,e^{-j2\pi l/N},\cdots,e^{-j2\pi l(N-1)/N}]$ and $\boldsymbol{J}_u=diag(H_u(0,k),H_u(1,k),\cdots,H_u(N-1,k))$. Let ω_u represent the summation of all squared absolute elements corresponding to user u in the squeezed signal part then it can be written as

$$\omega_u=\sum_{k\in u}\sum_{|l|\le\tau}\left|\sum_{n=0}^{N-1}b_nH_u(n,k)e^{j2\pi(\varepsilon_u-l)n/N}\right|^2$$

$$=\boldsymbol{b}^H\left(\sum_{k\in u}\boldsymbol{J}_u^H\boldsymbol{D}_u^HC(\boldsymbol{t})\boldsymbol{D}_u\boldsymbol{J}_u\right)\boldsymbol{b} \tag{26}$$

$\boldsymbol{t}=[1+2\tau,1+2\sum_{l=1}^{\tau}\cos 2\pi l/N,\cdots,1+2\sum_{l=1}^{\tau}\cos 2\pi(N-1)l/N]^T$.

Consequently, ε_s can be evaluated as

$$\varepsilon_s=\frac{\sigma_s^2}{N^2}\sum_{u=1}^{U}\omega_u \tag{27}$$

Assuming $\boldsymbol{\kappa}=diag(\boldsymbol{F}(\sigma_s^2\boldsymbol{A}\boldsymbol{A}^H+\sigma_z^2\boldsymbol{I})\boldsymbol{F}^H)$ and $\boldsymbol{\gamma}=\frac{\sigma_s^2}{N^2}\sum_{u=1}^{U}\sum_{k\in u}\boldsymbol{J}_u^H\boldsymbol{D}_u^H\boldsymbol{C}(\boldsymbol{t})\boldsymbol{D}_u\boldsymbol{J}_u$. The energy of the ICI plus noise part can be obtained as $\varepsilon_{in}=\boldsymbol{b}^H(\boldsymbol{\kappa}-\boldsymbol{\gamma})\boldsymbol{b}$. To optimize the vector $\boldsymbol{b}$, we use average SINR as the cost function, i.e.,

$$SINR(\boldsymbol{b})=\frac{\boldsymbol{b}^H\boldsymbol{\gamma}\boldsymbol{b}}{\boldsymbol{b}^H(\boldsymbol{\kappa}-\boldsymbol{\gamma})\boldsymbol{b}} \tag{28}$$

It is evident that the SINR is a generalized Rayleigh quotient form with respect to $\boldsymbol{b}$ and can be easily solved using eigenvalue decomposition. The optimal SINR is the largest eigenvalue of the matrix $(\boldsymbol{\kappa}-\boldsymbol{\gamma})^{-1}\boldsymbol{\gamma}$ and the corresponding vector $\boldsymbol{b}$ is the eigenvector associated with this largest eigenvalue [15]. A similar ICI squeezing algorithm for OFDM over doubly selective fading channels is proposed in [14]. This algorithm is designed for single user systems. In our scenario, mobile users may propagate through different wireless channels and incur distinct CFOs, leading to a more challenging problem.

Fig. 2 shows us that the post-SINR is obviously higher than the input signal-to-noise ratio (SNR), e.g., 4dB gain at low SNR region while 2.5dB at high SNR regime. Specifically, some performance gain is achieved after ICI squeezing preprocessing. We also note that this privilege is irrelevant to the users' mobile velocity, which implies that our proposed scheme is sufficiently robust in different mobile scenarios. In Section IV, BER performance in Fig. 5 explicitly validates our inference. Fig. 3 shows the effects of preprocessing the received multiuser signal on the amplitudes of ICI terms. Two cases are considered, in the first case the mobile velocity is 120km/h, while in the second it is 240km/h. The solid and dotted lines show the amplitudes of interference terms in the first column of the ICI matrix before and after ICI squeezing preprocessing for the first and second scenarios respectively. The gap of maximum to minimum power after ICI squeezing is approximately 70dB, while before preprocessing was 40dB. Similarly, same performance gain can be obtained with respect to different mobile cases. It can be observed that after preprocessing most power of the

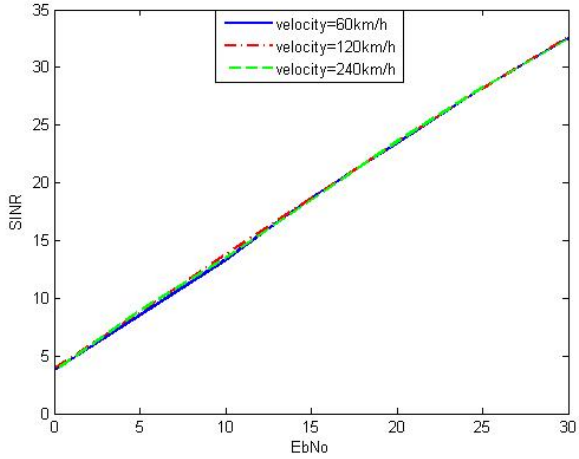

Fig. 2. SINR after the ICI squeezing preprocessing versus EbNo with respect to different mobile scenarios when $\tau=1$.

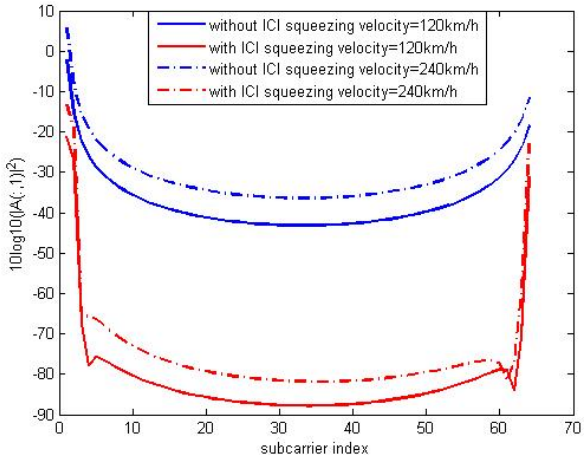

Fig. 3. The effect of ICI squeezing on the power of the interference terms with respect to different mobile scenarios when $\tau=1$ and $SNR=15dB$.

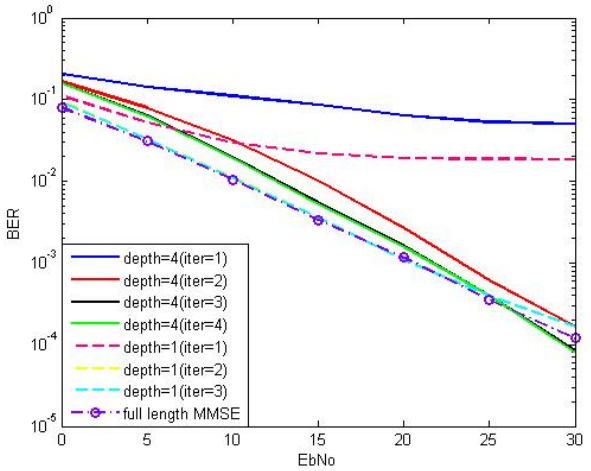

Fig. 4. BER comparison of the proposed scheme for different values of ICI squeezing depth and iteration number with the full length MMSE equalizer.

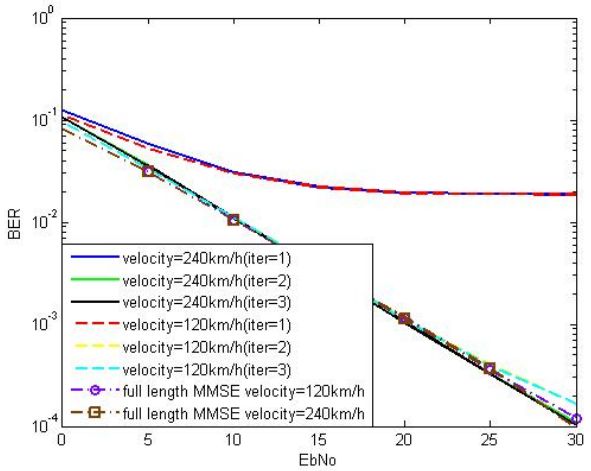

Fig. 5. BER comparison of the proposed scheme for different iteration number and velocity with the full length MMSE equalizer when $\tau = 1$.

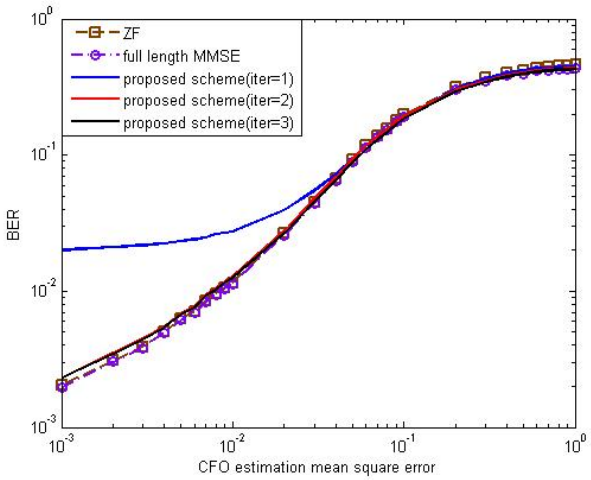

Fig. 6. BER comparison of the proposed scheme for different iteration number with the ZF and the full length MMSE equalizers versus CFO estimation mean square error when $\tau = 1$ and $SNR = 20dB$.

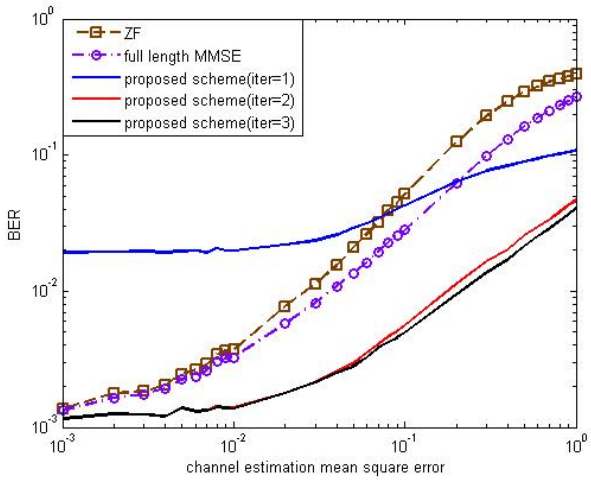

Fig. 7. BER comparison of the proposed scheme for different values of iteration number with the ZF and the full length MMSE equalizers versus channel estimation mean square error when $\tau = 1$ and $SNR = 20dB$.

interference is concentrated in the squeezed $2\tau+1$ ICI terms, which before preprocessing was spread in much more ICI terms. We also notice that the faster the terminal moves, the stronger the desired signal is, which indirectly explains the reason why the processing gain of ICI squeezing in different mobile scenarios is consistent. This can be attributed to a well known principle that the diversity is inversely proportional to the correlation of CIRs.

The data detection algorithm is similar as the iterative MMSE equalizer proposed in [14]. Specifically, the computational load of the shorten MMSE equalizer is dominated an $(2\tau+1)\times(2\tau+1)$ Hermitian matrix inversion. As this requires only $O(\tau^2)$ operations, a total of $O(N\tau^2)$ operations are needed per iteration. Besides, in order to obtain the preprocessing vector $\boldsymbol{\beta}$, we need to cauculate the eigenvector corresponding to the maximum eigenvalue of the generalized Rayleigh quotient problem (28) which entails $O(N)$ computations [16]-[17]. In contrast, the full length MMSE equalizer defined by (15) requires the inversion of an $N\times N$ ICI matrix, resulting in a prohibitively high complexity of $O(N^3)$.

IV. Simulation Results

We use a 64-subcarrier 4-user fully loaded OFDMA system, where the OFDM symbol length T is $6.4\times10^{-5}s$. Subcarriers are assigned to users in an interleaved fashion and BPSK is deployed as the modulation scheme. Four users encounter independent doubly selective three-ray Rayleigh fading channels and the multipath intensity profile experiences an exponential distribution. Unless otherwise mentioned, the four users' CFOs are taken to be 0.15, -0.1, 0.2 and 0.1, the users' mobile velocity relative to the BS is assumed to be 120km/h as indicated in the IEEE 802.16e standard. The maximum Doppler shift is calculated based on a carrier frequency of $f_c = 2GHz$. For comparison, the performance of the full length MMSE equalizer derived by Hou [12] is plotted as a benchmark.

As indicated in [8], the appropriate choice of τ mainly depends on the maximum normalized CFO from any user, denoted as α. In such a scenario the transmitted symbol at subcarrier k can be drifted to $k\pm\alpha$ subcarriers. Therefore, to estimate the transmitted symbol at subcarrier k, subcarriers

from $k-\alpha$ to $k+\alpha$ need to be incorporated into the squeezed signal part. Hence the value of τ in our case should be equal to 1. Fig. 4 illustrates us the BER performance of the proposed scheme for different values of ICI squeezing depth and iteration number versus SNR. It is observed that with $\tau=1$ the proposed algorithm converges fast in two iterations and its performance approaches that of the full length MMSE equalizer but with a significant reduction on computational complexity from $O(N^3)$ to $O(N)$. As mentioned above, due to the simulation parameters we select, the ICI squeezing scheme with $\tau=1$ yields better performance than with $\tau=4$ which requires three iterations to converge and is 2.5dB away from the bound at low SNR region. The reason for this phenomenon is that after ICI squeezing preprocessing, the shortened equalizer with $\tau=4$ utilizes more received samples than necessary, thus incurring more estimation noise.

Fig. 5 shows us the BER performance of the proposed algorithm in different mobile scenarios versus various SNR values. As expected, the BER curves generated by different mobile velocities are overlapped with each other and converge in two iterations. Again, their performances are the same as the full length MMSE equalizer. By using the proposed detection scheme, the strict requirement on the limit of mobile speed, such as the 120km/h stated in IEEE 802.16e standard, can be dramatically relaxed.

In practice, inevitable channel and CFOs estimation errors will affect the detection performance. To study the performance of the proposed detection technique in the presence of erroneous channel and CFOs estimations, we model the estimation errors as independent white Gaussian random variables. We simulate the average BER against the channel and CFOs estimation MSE when $\tau=1$ and $SNR=20dB$ and present the results in Fig. 6 and Fig. 7 respectively. As can be seen in Fig. 6, the proposed scheme with two iterations can still exhibit satisfactory performance as that of ZF and MMSE equalizers in this scenario. Clearly in Fig. 7, our algorithm with two iterations has insignificant performance loss until the channel estimation errors exceed 0.01, which is a relatively large value in channel estimation. In contrast, ZF and MMSE equalizers are more sensitive to the channel estimation errors compared with our method. It is seen that the proposed detection technique with two iterations yields better performance than the full length MMSE equalizer in such an erroneous environment and ZF algorithm gives the worst performance. This gain is further elevated as the MSE of channel estimation increases. This phenomenon can be attributed to the fact that MMSE and ZF equalizers need all the received samples to do detection, thus more sensitive to estimation error than the shortened equalizer which only employs limited samples to decode. In contrast, the evaluated schemes suffer almost the same in the erroneous CFO scenario since MUI is mainly introduced by neighboring subcarriers. We also notice that more iterations are needed to ameliorate the system performance when large deviation is present. This result shows that the proposed scheme is sufficiently robust to the channel estimation errors that arise from practical implementation.

V. CONCLUSION

In this paper, we design an ICI squeezing approach via fast convolution for OFDMA uplink over time and frequency selective fading channels, which consequently renders the interference matrix a banded structure and dramatically reduce the detection complexity by employing a shortened MMSE equalizer. The iterative detection scheme converges very fast and is sufficiently robust to different mobile scenarios and channel estimation errors. Simulation results show that the proposal is able to give reliable BER performance in practical environment and approaches that of the full length MMSE equalizer, facilitating its application in future wireless communication systems.

REFERENCES

[1] M. Morelli, "Timing and frequency synchronization for the uplink of an OFDMA system," *IEEE Trans. Commun.*, vol. 52, no. 2, pp. 296-306, Feb. 2004.

[2] A. M. Tonello and S. Pupolin, "Performance of single user detectors in multitone multiple access asynchronous communications," in *Proc. IEEE VTC 2002-Spring*, Birmingham, Alabama, USA, May 2002, pp. 199-203.

[3] J. Choi, C. Lee, H. W. Jung, and Y. H. Lee, "Carrier frequency offset compensation for uplink of OFDM-FDMA systems," *IEEE Commun. Lett.*, vol. 4, no. 12, pp. 414-416, Dec. 2000.

[4] R. Fantacci, D. Marabissi, and S. Papini, "Multiuser interference cancellation receivers for OFDMA uplink communications with carrier frequency offset," in *Proc. IEEE Globecom 2004*, Dallas, Texas, USA, Dec. 2004, pp. 2808-2812.

[5] D. Huang and K. B. Letaief, "An interference-cancellation scheme for carrier frequency offsets correction in OFDMA systems," *IEEE Trans. Commun.*, vol. 53, no. 7, pp. 1155-1165, Jul. 2005.

[6] D. Sreedhar and A. Chockalingam, "MMSE receiver for multiuser interference cancellation in uplink OFDMA," in *Proc. IEEE VTC 2006-Spring*, Melbourne, Australia, May 2006, pp. 2125-2129.

[7] M. Morelli, C. C. J. Kuo, and M. O. Pun, "Synchronization techniques for orthogonal frequency division multiple access (OFDMA): a tutorial review," *IEEE Proceedings*, vol. 95, no. 7, pp. 1394-1427, Jul. 2007.

[8] Z. Cao, U. T'ureli, and Y. Yao, "Low-complexity orthogonal spectral signal construction for generalized OFDMA uplink with frequency synchronization errors," *IEEE Trans. Veh. Technol.*, vol. 56, no. 3, pp. 1143-1154, May 2007.

[9] Z. Cao, U. T'ureli, and Y. Yao, "Analysis of two receiver schemes for interleaved OFDMA uplink," in *Proc. IEEE ACSSC 2002*, Monterey, California, USA, Nov. 2002, pp. 1818-1821.

[10] C. Y. Hsu and W. R. Wu, "A low-complexity zero-forcing CFO compensation scheme for OFDMA uplink systems," *IEEE Trans. Wireless Commun.*, vol. 7, no. 10, pp. 3657-3661, Oct. 2008.

[11] D. Galda, H. Rohling, and E. Costa, "On the effects of user mobility on the uplink an OFDMA system," in *Proc. IEEE VTC 2003-Spring*, Jeju, Korea, Apr. 2003, pp. 1433-1437.

[12] S. W. Hou and C. C. Ko, "Intercarrier interference suppression for OFDMA uplink in time and frequency selective fading channels," *IEEE Trans. Veh. Technol.*, vol. 58, no. 6, pp. 2741-2754, Jul. 2009.

[13] P. Sun and L. Zhang, "Low complexity pilot aided frequency synchronization for OFDMA uplink transmission," *IEEE Trans. Wireless Commun.*, vol. 8, no. 7, pp. 3758-3769, Jul. 2009.

[14] P. Schniter, "Low-complexity equalization of OFDM in doubly selective channels," *IEEE Trans. Signal Process.*, vol. 52, no. 4, pp. 1002-1011, Apr. 2004.

[15] X. Zhang, *Matrix Analysis and Application*. Beijing, China: Tsinghua Univ. Press, 2004.

[16] G. H. Golub and C. F. V. Loan, *Matrix Computations, 3rd Edition*. Baltimore, Maryland, USA: Johns Hopkins Univ. Press, 1996.

[17] S. Ahmed and L. Zhang, "Low complexity iterative detection for OFDMA uplink with frequency offsets," *IEEE Trans. Wireless Commun.*, vol. 8, no. 3, pp. 1199-1205, Mar. 2009.